UC Irvine
UC Irvine Previously Published Works

Title

Current estimates of biogenic emissions from eucalypts uncertain for southeast Australia

Permalink

https://escholarship.org/uc/item/9d38t019

Journal

Atmospheric Chemistry and Physics, 16(11)

ISSN

1680-7316

Authors

Emmerson, Kathryn M
Galbally, Ian E
Guenther, Alex B
et al.

Publication Date

2016

DOI

10.5194/acp-16-6997-2016

Copyright Information

Peer reviewed

Atmospheric
Chemistry
and Physics

Current estimates of biogenic emissions from eucalypts uncertain for southeast Australia

Kathryn M. Emmerson[1], **Ian E. Galbally**[1], **Alex B. Guenther**[2], **Clare Paton-Walsh**[3], **Elise-Andree Guerette**[3], **Martin E. Cope**[1], **Melita D. Keywood**[1], **Sarah J. Lawson**[1], **Suzie B. Molloy**[1], **Erin Dunne**[1], **Marcus Thatcher**[1], **Thomas Karl**[4], **and Simin D. Maleknia**[5]

[1]CSIRO Oceans & Atmosphere, PMB1, Aspendale, VIC, Australia
[2]Department of Earth System Science, University of California, Irvine, USA
[3]Centre for Atmospheric Chemistry, School of Chemistry, University of Wollongong, Wollongong, NSW, Australia
[4]Institute of Atmospheric and Cryospheric Sciences, University of Innsbruck, Innsbruck, Austria
[5]Centre for Ecosystem Science, School of Biological, Earth and Environmental Sciences,
University of New South Wales, Sydney, Australia

Correspondence to: Kathryn M. Emmerson (kathryn.emmerson@csiro.au)

Abstract. The biogenic emissions of isoprene and monoterpenes are one of the main drivers of atmospheric photochemistry, including oxidant and secondary organic aerosol production. In this paper, the emission rates of isoprene and monoterpenes from Australian vegetation are investigated for the first time using the Model of Emissions of Gases and Aerosols from Nature version 2.1 (MEGANv2.1); the CSIRO chemical transport model; and atmospheric observations of isoprene, monoterpenes and isoprene oxidation products (methacrolein and methyl vinyl ketone). Observations from four field campaigns during three different seasons are used, covering urban, coastal suburban and inland forest areas. The observed concentrations of isoprene and monoterpenes were of a broadly similar magnitude, which may indicate that southeast Australia holds an unusual position where neither chemical species dominates. The model results overestimate the observed atmospheric concentrations of isoprene (up to a factor of 6) and underestimate the monoterpene concentrations (up to a factor of 4). This may occur because the emission rates currently used in MEGANv2.1 for Australia are drawn mainly from young eucalypt trees (< 7 years), which may emit more isoprene than adult trees. There is no single increase/decrease factor for the emissions which suits all seasons and conditions studied. There is a need for further field measurements of in situ isoprene and monoterpene emission fluxes in Australia.

1 Introduction

Biogenic volatile organic compounds (BVOCs) originate from terrestrial and marine ecosystems, and have an annual flux of approximately $1150\,\mathrm{Tg\,C\,yr^{-1}}$ (Guenther et al., 1995). Almost 90 % of BVOCs are emitted from plants and trees, with the most dominant species being isoprene and monoterpenes (Lathière et al., 2006; Guenther et al., 2012). The isoprene and monoterpene emission rates from vegetation are determined by a combination of environmental factors (light, temperature, water stress etc.) and genetic make-up of the species being considered (Guenther et al., 2012). In regions of dense vegetation these BVOCs dominate the oxidative capacity of the atmosphere (Houweling et al., 1998; Taraborrelli et al., 2012) and are important in the production of ozone (Simpson, 1995; Pierce et al., 1998) and secondary organic aerosol (Hoffmann et al., 1997; Griffin et al., 1999; van Donkelaar et al., 2007).

Concentrations of BVOCs in the atmosphere are a function of the emission rate from the underlying vegetation, the mixing depth of the boundary layer, entrainment rate at the top of the boundary layer, horizontal advection, the rate of removal within the boundary layer by the hydroxyl and nitrate radicals, and ozone. All of these processes vary diurnally. Modern chemical transport models can simulate all these processes provided they include an emission module

for BVOCs such as the Model of Emissions of Gases and Aerosols from Nature (MEGAN).

MEGAN was developed to provide a parameterisation for BVOC emissions applicable over the Earth's surface (Guenther et al., 2012, 2006, 1995). MEGAN uses meteorological parameters such as temperature and solar radiation, land use maps incorporating vegetation and land cover, and emission factors based on global observations of plant responses to light and temperature. MEGAN has been incorporated and run within a number of global chemistry models (Guenther et al., 2006; Heald et al., 2008; Emmons et al., 2010; Millet et al., 2010; Pfister et al., 2008) and for regional air quality studies (Situ et al., 2013; Stavrakou et al., 2014; Kim et al., 2014). Sensitivity studies on the input data for MEGAN have highlighted the importance of time and spatial resolution in meteorological data (Ashworth et al., 2010; Arneth et al., 2011). A comparison of isoprene emissions driven by low-resolution (degree scale) and high-resolution (10 km) meteorological fields showed changes up to 150 % due to smoothing via averaging effects (Pugh et al., 2013). The importance of using accurate land cover data with respect to the effects of isoprene on ozone concentrations has also been discussed (Kim et al., 2014), as has changing all vegetation from default species to eucalypts (Situ et al., 2013), which increased isoprene concentrations by 315 %.

There are over 700 species of eucalypts native to Australia, many of which are expected to contribute to isoprene emissions in the southeast region. Evans et al. (1982) reported the first comprehensive survey of isoprene emission and found that *Eucalyptus globulus* was the highest isoprene emitter of the 54 plant species examined. Eucalypts were selected to be the subject of a number of subsequent isoprene emission studies and are considered as among the highest isoprene-emitting plants (e.g. Loreto and Delfine, 2000). A small number of BVOC emission measurements have been made in Australia, particularly of eucalypt species (Winters et al., 2009; He et al., 2000), flowering plants and pasture, including grass cutting (Kirstine et al., 1998) and tropical grasslands/woodlands (Ayers and Gillett, 1988). Emissions from eucalypt species outside Australia have been measured in the field (Street et al., 1997) and the laboratory (Guenther et al., 1991).

Previous MEGAN predictions of BVOC emissions across Australia have had limited success. Müller et al. (2008) found an overestimate of isoprene across northern Australia by comparing MEGANv2 to GOME satellite measurements of formaldehyde, and subsequently Stavrakou et al. (2015) estimated the magnitude of this over-prediction to be a factor of 2–3 in January. Sindelarova et al. (2014) found that reductions of 50 % in Australian isoprene emissions could be achieved by accounting for reduced isoprene emissions during low soil moisture conditions.

The imperative for understanding biogenic emissions from Australia is clear as the country covers 22 % of the land area in the Southern Hemisphere (excluding Antarctica). This is the first high-resolution regional study focussing on whether the emission factors used in MEGAN are appropriate to represent BVOC emissions from diverse locations in southeast Australia. We compare atmospheric concentrations of isoprene and monoterpenes observed in these locations with concentrations modelled using MEGAN, the default emission factors and the CSIRO chemical transport model. Sensitivity studies are undertaken on these emission factors. Tests on other variables to assess model uncertainty are shown in the Supplement. Differences between the modelled and measured BVOCs are critically examined and the need for revised regional emission factors is evaluated.

2 Materials and methods

2.1 Field experiments

Gas-phase biogenic VOC data were measured using a proton transfer reaction mass spectrometer (PTR-MS); data were collected during four field experiments in areas of diverse land cover in southeast Australia. Figure 1 shows a map giving the locations of the field campaign sites in southeast Australia, showing their proximity to the coast and urban regions, as well as forested areas. Data within Fig. 1 are discussed later. The PTR-MS measures groups of species which correspond to certain mass-to-charge (m/z) ratios; for example, isoprene, C_5H_8, is identified at $m/z = 69$ (made up of the mass of C_5H_8, $68\,g\,mol^{-1}$, and a proton, $1\,g\,mol^{-1}$). Whilst monoterpenes are identified at both $m/z = 137$ and 81 (a dominant fragment produced by dissociative proton transfer), only the $m/z = 137$ will be used. The PTR-MS technique is ideal for developing and evaluating parameterisations for lumped species modelling as most chemical mechanisms do not separate individual monoterpenes such as α- and β-pinenes, and conventional gas chromatographic techniques may underestimate the actual monoterpene loading (Lee et al., 2005). Hourly averages have been calculated from the PTR-MS data to be comparable to the time period of the modelled output. For details of the PTR-MS measurements please refer to the citations given for each field campaign.

2.1.1 The Sydney Particle Study

The Sydney Particle Study (SPS) took place at Westmead, 33 km to the west of central Sydney (150.9961° E, 33.8014° S) (Cope et al., 2014). The site is situated in a grassy field within the grounds of a psychiatric hospital. Two intensive field campaigns took place, occurring between 1 February and 7 March 2011 (SPS1, summer) and 14 April and 14 May 2012 (SPS2, autumn). The PTR-MS was operational from 18 February during SPS1 and throughout the whole of SPS2. The height of the inlet was approximately 4 m.
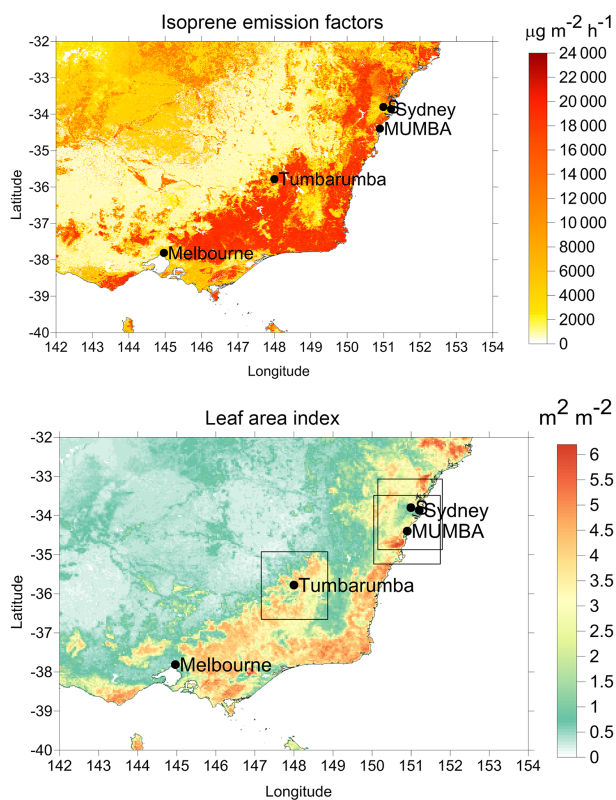
Figure 1. Southeast Australia at 1 km resolution, showing (top) isoprene from the MEGAN global emission factor map and (bottom) LAI in January, with the boundaries of the inner model domains marked. Major cities and the field campaign locations are also shown. The Sydney field campaigns were located west of the Sydney marker.

2.1.2 MUMBA

The Measurement of Urban, Marine and Biogenic Air (MUMBA) field campaign took place between 21 December 2012 and 16 February 2013 (summer) at the University of Wollongong eastern campus (150.8995° N, 34.3972° S), about 80 km to the south of Sydney (Paton-Walsh et al., 2016). Wollongong is a coastal location with sharp gradients between marine, urban and forested regions. The PTR-MS instrument was situated in a hut surrounded by a grass field and was sampled from a mast at a height of ~ 10 m above the surrounding ground level.

2.1.3 Tumbarumba

PTR-MS measurements were made for one week at Tumbarumba in New South Wales (148.1517° E, 35.6566° S) between 8 and 14 November 2006 (late spring) (Maleknia, 2012; Maleknia et al., 2009). Tumbarumba is located within the Bago State Forest and is surrounded by dominant eucalypt species of *E. delegatensis* (alpine ash) and *E. dalrympleana* (mountain gum) with an average height of 40 m. Iso-

prene and monoterpenes were observed from an inlet height of 45 m. Despite being performed in late spring, the campaign experienced snowstorm conditions that caused damage to the trees. This resulted in a 4-fold increase in the emissions of monoterpenes, whilst isoprene levels remained low due to cold temperatures (~ 8 °C) (Maleknia et al., 2009). Three days of eddy covariance flux measurements are available for isoprene and monoterpenes from the post-storm period at Tumbarumba. These data will provide a direct constraint on modelled emissions despite being caveated by the unusual vegetation stress response.

2.2 The modelling framework

The CSIRO Chemical Transport Model (CTM) has been developed over 15 years for Australian regional air quality issues (Cope et al., 2004). The CTM is a three-dimensional Eulerian chemical transport model with 35 levels in the vertical to 40 km. The CTM has the capability of modelling the emissions, transport, chemical transformation, and wet and dry deposition of a coupled gas- and aerosol-phase atmospheric system. The modelling uses a nested approach, downscaling from global background concentrations which are advected into the Australian region by the prevailing winds. The Australia-wide domain at 80 km resolution is used to simulate the transport of species from large-scale continental processes that feed into the boundary conditions of three successively smaller nested grids. The highest resolution grid (3 km) has a domain size of 180 km × 180 km and is centred on each field campaign site.

The CTM is driven by meteorology from the Conformal Cubic Atmospheric Model (CCAM; McGregor and Dix, 2008). CCAM is a global stretched grid dynamical model, used for the prediction of wind velocity, temperature, water vapour mixing ratio (including clouds), radiation and turbulence. CCAM has been evaluated for use in Australia and elsewhere (Corney et al., 2013; Nguyen et al., 2014). CCAM uses the Australian land surface scheme, CABLE (Kowalczyk et al., 2013), to provide information on the surface roughness, soil moisture and leaf area index (LAI, based on MODIS data). The soil moisture parameter has been evaluated indirectly within the Global Soil Wetness Project by comparing model evapotranspiration and runoff to measurements (Zhang et al., 2013). Whilst CABLE performed well, soil moisture remains a source of uncertainty.

We have included MEGAN as an option in the CTM to calculate the biogenic emissions, the setup of which is described below. Anthropogenic emissions are based on the Sydney Greater Metropolitan Region inventory (NSW Department of Environment, Climate Change and Water, now NSW EPA; DECCW, 2007) and includes 37 species. The chemical transformation of gas-phase species is modelled using an extended version of the Carbon Bond 5 mechanism (Sarwar et al., 2008) with updated toluene chemistry (Sarwar et al., 2011). The CB05 mechanism treats the production

Table 1. Model setup and list of model runs completed.

	SPS1	SPS2	MUMBA	Tumbarumba
240 h average temperature, K	295	290	295	289
24 h average PAR, μmol m^{-2} s^{-1}	437	305	485	500
Coarse grid PFT	X			
Base MEGAN run	X	X	X	X
Exchange 50 % crops $\rightarrow$ grass				X
Emission factors isoprene / 3 monoterpenes $\times$ 3.5	X	X	X	X
$\pm$20 % NO$_x$ emissions*	X	X	X	X

* Shown in Supplement.

of a lumped isoprene oxidation product only, simplifying the chemistry. More recent schemes consider explicit oxidation products which can affect the production of ozone and nitrate species. The CB05 mechanism and its predecessor, CBIV, have been compared with other schemes in Emmerson and Evans (2009) and Knote et al. (2015), but not against measurements. The choice of chemistry scheme can introduce uncertainty, which could be explored in future work. A two-bin sectional scheme calculates the aerosol concentrations, using the volatility basis set (Shrivastava et al., 2008) for the secondary organic species partitioning, and ISORROPIA (Fountoukis and Nenes, 2007) for the inorganic partitioning. The CTM runs on a chemical time step of 5 min with hourly output of all variables. Table 1 details how the model has been set up and run, along with particulars of the sensitivity runs completed.

2.3 Coupling MEGAN to the CSIRO CTM

MEGAN was developed to provide a parameterisation for BVOC emissions, and detailed descriptions can be found in Guenther et al. (2012), with a useful review of modules given in Sindelarova et al. (2014). The most recent version, MEGANv2.1, includes 147 species in 19 BVOC classes, which can be output into lumped species appropriate for a number of popular chemical mechanisms, including the Carbon Bond 5 mechanism.

MEGANv2.1 is available as an offline code at http://lar.wsu.edu/megan/guides.html. The code is set up for use with the Weather Research and Forecasting (WRF) modelling system, but it does not include the effect of CO_2 on isoprene (Heald et al., 2009) or the effects of soil moisture. Note that soil moisture is used elsewhere in the CTM to calculate the dust emission flux and could be coupled with MEGAN in the future. In this work, the MEGANv2.1 code has been extracted from the WRF system and coupled to the CSIRO CTM.

MEGANv2.1 provides two approaches for estimating emission factors. The first is to use the 16 plant functional type (PFT) distributions and the global average PFT-specific emission factors listed in Table 2 of Guenther et al. (2012). In this case the emission rate, R (μg m^{-2} h^{-1}), of species i in

any grid box will be sensitive to the PFT distributions used for the MEGAN simulation (Eq. 1):

$$R_i = \sum_{j=1}^{nPFT} \left(\text{EF}_{ij} \times \gamma_{ij} \times \chi_j \right), \tag{1}$$

where EF_{ij} is the emission factor (μg m^{-2} h^{-1}) of species i under standard conditions for PFT j with fractional grid box areal coverage χ_j. The emission activity factor γ_{ij} (dimensionless) accounts for emission control processes and uses the following variables to drive the canopy model: compound class, response to light and temperature, leaf age, soil moisture, CO_2 and LAI.

The second approach is to use MEGAN global emission factor maps, which are based on plant type composition and plant-type-specific emission factors. In this case, the MEGAN simulation uses PFTs to define the canopy environment characteristics and to define the fractional grid box areal coverage, but the results are not as sensitive to the PFT data used. The emission rate, R, for species i in a given grid cell, xy, is (Eq. 2)

$$R_i = \text{EF}_{i,xy} \sum_{j=1}^{nPFT} \left(\gamma_{ij} \times \chi_j \right). \tag{2}$$

This study uses both approaches, the latter approach for 10 species where emission factor maps are available, and the former approach for all other species. Global emission factor maps (version 2011) for isoprene, myrcene, sabinene, limonene, 3-carene, ocimene, α-pinene, β-pinene, 232-MBO (2-methyl-3-buten-2-ol) and NO are provided at a 1 km resolution with the MEGANv2.1 code download and are described below.

2.3.1 Production of emission factor maps for Australia

The MEGANv2.1 emission factor maps provide values for a specific location based on estimates of plant type composition, which can be individual plant species or more general types, and emission factors for each plant type. The global MEGAN PFT database was used to quantify the fraction of trees, shrubs, crops and herbs at each location

in Australia. The tree/shrub type composition for Australia was then determined from data compiled by the Australian Department of Agriculture and Water Resources (DAWR) and released on the data.gov.au data portal in 2003 (URL: http://data.gov.au/dataset/forests-of-australia-2003, DAWR, 2003). The DAWR land cover data are representative of the time period of 1996 to 2002 and include 20 categories. Australia has unusually low tree/shrub genera diversity and many of these landscapes were represented in the DAWR database by a single tree/shrub genera (e.g. *Acacia*, *Callitris*, *Casuarina*, *Eucalyptus*, *Melaleuca*) although some were more diverse (mangrove, rainforest). The landscapes dominated by one genera were assigned the genera average emission factor in the MEGAN plant type database. Mixed landscapes were assigned a representative plant type (e.g. the emission factor for the genera *Avicennia* was assigned to trees in the mangrove landscape).

The MEGANv2.1 emission factor database classifies *Eucalyptus* as a high emitter ($> 10 \,\mu g \, g^{-1} \, h^{-1}$), *Casuarina* and *Melaleuca* as moderate emitters (1–$10 \,\mu g \, g^{-1} \, h^{-1}$), and *Avicennia* and *Callitris* as very low emitters ($< 1 \,\mu g \, g^{-1} \, h^{-1}$). Isoprene or monoterpene emissions have not been published for any Australian acacias, but eight acacia species from South Africa (Guenther et al., 1996; Harley et al., 2003) and the US (Guenther et al., 1999; Papiez et al., 2009) have been investigated and only one isoprene emitter and one monoterpene emitter have been identified. Based on these observations, the MEGAN model assumes low isoprene and monoterpene emission rates for Australian acacia species. The MEGANv2.1 isoprene emission factor for *Eucalyptus* was based on six enclosure measurement studies (Evans et al., 1982; Winer et al., 1983; Guenther et al., 1991; Street et al., 1997; Loreto and Delfine, 2000; He et al., 2000). Of these studies, only He et al. (2000) was conducted in Australia. These studies report a large range of emission rates that are equivalent to MEGAN landscape emission factors of 1.6 to $51 \, mg \, g^{-1} \, h^{-1}$. Large variability (more than a factor of 3) was observed for different plants of the same eucalypt species measured in a single study (Guenther et al., 1991). The average isoprene emission factor of 15 eucalypt species measured by He et al. (2000), about $24 \, mg \, m^{-2} \, h^{-1}$, was similar to the mean value for the other five studies and used as the basis for assigning eucalypts an isoprene emission factor of $24 \, mg \, m^{-2} \, h^{-1}$. This is more than double the isoprene emission factor used for broadleaf evergreen temperate trees if approach 2 is used (PFT-sensitive).

The distribution of isoprene emission factors in southeast Australia is shown in Fig. 1a. The region between Melbourne and Sydney is covered in vegetation emitting at the upper end of the map scale, close to $24 \, mg \, m^{-2} \, h^{-1}$.

2.3.2 Meteorological and related inputs to MEGAN

The MEGAN canopy model requires photosynthetically active radiation (PAR), temperature, pressure, relative humidity and LAI. CCAM supplies hourly temperature and PAR, which exhibit diurnal cycles with early afternoon maxima. The hourly PAR is reduced by a cloud attenuation factor when conditions are cloudy. MEGAN also requires an estimate of previous growing conditions and needs 24 and 240 h averaged temperature and PAR. The 24 h average of temperature is provided by CCAM. The 240 h averaged temperature is fixed at the observed average temperature for the duration of each campaign. The 24 h averaged PAR is set using measured solar radiation (in $W \, m^{-2}$) rather than CCAM output when measurements were available during the SPS2 and MUMBA campaigns. The observed and modelled PAR from the respective receptor sites is presented in Fig. 2. This calculation assumes PAR is half the total solar radiation fraction in the 400–700 nm wavelength band, and the conversion factor from $W \, m^{-2}$ to $\mu mol \, m^{-2} \, s^{-1}$ is 4.5. The model predicts the correct shape of the diurnal profile but over-predicts by $126 \,\mu mol \, m^{-2} \, s^{-1}$ (7 %) at noon during summer (MUMBA) and under-predicts by $236 \,\mu mol \, m^{-2} \, s^{-1}$ (25 %) during autumn (SPS2). Average campaign-modelled PAR is used for SPS1 and Tumbarumba. Values for temperature and PAR are given in Table 1.

LAI data are provided from CCAM as described, at the same resolution as each model grid. The distribution of LAI in summer (January) is shown in Fig. 1b, with high LAI data in the region of 5–6 $m^2 \, m^{-2}$ in the coastal plains and mountain ranges of southeast Australia.

2.3.3 Construction of high-resolution PFT map for Australia

The Community Land Model PFT data from the NCAR data repository is provided on a $0.5° \times 0.5°$ resolution, which when downscaled to the inner 3 km grids for the CSIRO-CTM is not suitable (shown in Sect. 3.2). A new PFT dataset has been constructed for this work, as 3 km resolution data in the same format as the 16 PFTs required by MEGAN are not available. A dataset from the International Geosphere-Biosphere Project (IGBP) available at a resolution of 1 km with 17 land cover types (Belward et al., 1999) was used. The IGBP dataset was converted into NCAR PFTs based on the schemes of Bonan et al. (2002) and Poulter et al. (2011) and local knowledge. Bonan et al. (2002) suggest how much bare ground should be introduced to each PFT grid cell, and also how best to split the boreal from the temperate and tropical plant types using the average temperature of the coldest month. A 30-year climatology of observed average winter temperatures (June–August) in Australia from the Bureau of Meteorology was used for this purpose (http://www.bom.gov.au/jsp/awap/, BoM, 2009).

Poulter et al. (2011) noticed that the IGBP classified much of Australia's interior with open shrublands. As a result, "shrublands", "grasslands" and "savannahs" were split into a combination of shrubs and grass as per their implementation in CABLE. Neither Bonan et al. (2002) nor CABLE have
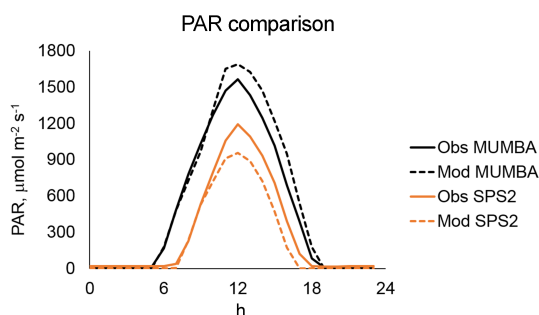
PAR comparison

Figure 2. Comparison of photosynthetically active radiation for modelled and measured SPS2 and MUMBA data.

vegetation occurring within "urban" land cover types, which would lead to zero biogenic VOC emissions in Sydney within this high-resolution implementation. An estimate of vegetation cover in Australian urban areas was made based on Kirstine and Galbally (2004). Table S1 in the Supplement gives details of how the IGBP land cover dataset was split into the NCAR 16 PFTs suitable for MEGAN. Figure 3 shows the resulting spatial extent of the PFTs that contribute at the field campaign sites. The maps show a high density (in most cases 95 % coverage) of broadleaf evergreen temperate trees around the coastal area. Shrubs and grasslands dominate the northwest region, with crops dominating the area in between.

3 Results

3.1 Contribution of plant functional types to emissions

We calculate the isoprene and monoterpene emission rates per plant functional type for each field campaign's inner nested grids in the model (180 km × 180 km). The SPS and MUMBA grids are coastal and therefore contain a high percentage of zero-emitting ocean squares. The bar chart in Fig. 4 shows that the emission rate for isoprene is an order of magnitude more than monoterpenes and that broadleaf evergreen temperate trees dominate all campaign airsheds. Tumbarumba is located near an agricultural region and is influenced by emissions from crops, though whether these are croplands or pasture for animals is uncertain. The combination of high emission factors and percentage of broadleaf evergreen temperate trees in the Tumbarumba grid (eucalypts, Sect. 2.1.3) enables up to $3.2\,\mu g\,m^{-2}\,h^{-1}$ of isoprene to be emitted (which includes crop PFTs). A sensitivity study conducted for Tumbarumba transferred 50 % of the crop area to grassland. This resulted in reducing the peak isoprene by 0.5–0.7 ppb but did not affect the monoterpene concentrations.

3.2 Comparisons of modelled and observed BVOCs

Observed and modelled isoprene and monoterpenes are presented as time series for the four field campaigns in Fig. 5.

Modelled isoprene is mostly over-predicted and monoterpenes are mostly under-predicted. The model captures the general peaks and troughs in the data, but at the wrong magnitude.

There are missing data from the observed SPS1 dataset and it is not obvious whether observed concentrations would have risen further on 18–19 February 2011 as the model suggests. Also shown on the SPS1 time series (Fig. 5 top plots) are the results using the coarse $0.5° \times 0.5°$ resolution PFT map. The very low concentrations of isoprene (peak of 0.2 ppb) show that resolution of the input data is important, and recreating the PFT maps was necessary.

Two of the first three modelled isoprene peaks in the MUMBA dataset (Fig. 5 third plots down) coincide with very hot (> 40 °C) measured days. The first modelled isoprene peak on 8 January is 38 ppb at 43 °C, yet the observed peak is 5 ppb at 41 °C. There may be isoprene inhibition at temperatures in excess of 40 °C which is not represented by the model (Guenther et al., 1991). January 8 is the only day CCAM predicts above 40 °C during MUMBA, whilst observations on 8 and 18 January are also above 40 °C. CCAM predicts 33 °C on 18 January, leading to modelled isoprene of 7 ppb; the observations show 4.5 ppb at 44 °C. The modelled peak of 8 ppb at 32 °C on 12 January is not mirrored by an observed peak. Whilst temperatures were hot throughout NSW on 12 January, a sea breeze kept Wollongong cooler at 25 °C. The modelled monoterpene Tumbarumba dataset has a number of peaks not seen in the observations (Fig. 5 bottom plots).

Figure 6 shows the eddy covariance flux measurements of isoprene and monoterpenes from the post-storm period at Tumbarumba. Uncertainty in the night-time observations are 40 % because advection terms were not well constrained; however, the daytime fluxes that dominate are within typical levels of uncertainty. The observed diurnal cycles are compared to modelled emission flux data for the same time period in Fig. 6. These observations show peak monoterpene fluxes under $0.8\,mg\,m^{-2}\,h^{-1}$ at a time when the monoterpene response increased by a factor of 4 as a result of the storm (Maleknia et al., 2009). Observed isoprene fluxes peak under $0.2\,mg\,m^{-2}\,h^{-1}$. The midday modelled emission rates over-predict the observed isoprene fluxes by a factor of 3 and under-predict the monoterpene fluxes by a factor of 4. Comparing the emission fluxes directly gives confidence that the modelled discrepancy is principally due to the emissions rather than model transport or chemical processes (shown in the Supplement).

Calculated ratios of emitted isoprene to monoterpene carbon were found to be 26.4 for forests in Michigan (Kanawade et al., 2011) and 15.2 in the Amazon (Greenberg et al., 2004), both of which are isoprene-dominated, whilst forests in Finland (ratio = 0.18) are dominated by monoterpenes (Spirig et al., 2004). These Tumbarumba data show a ratio of 0.14, highlighting the monoterpene dominance after the storm. If the storm had not taken place, we suggest that isoprene and
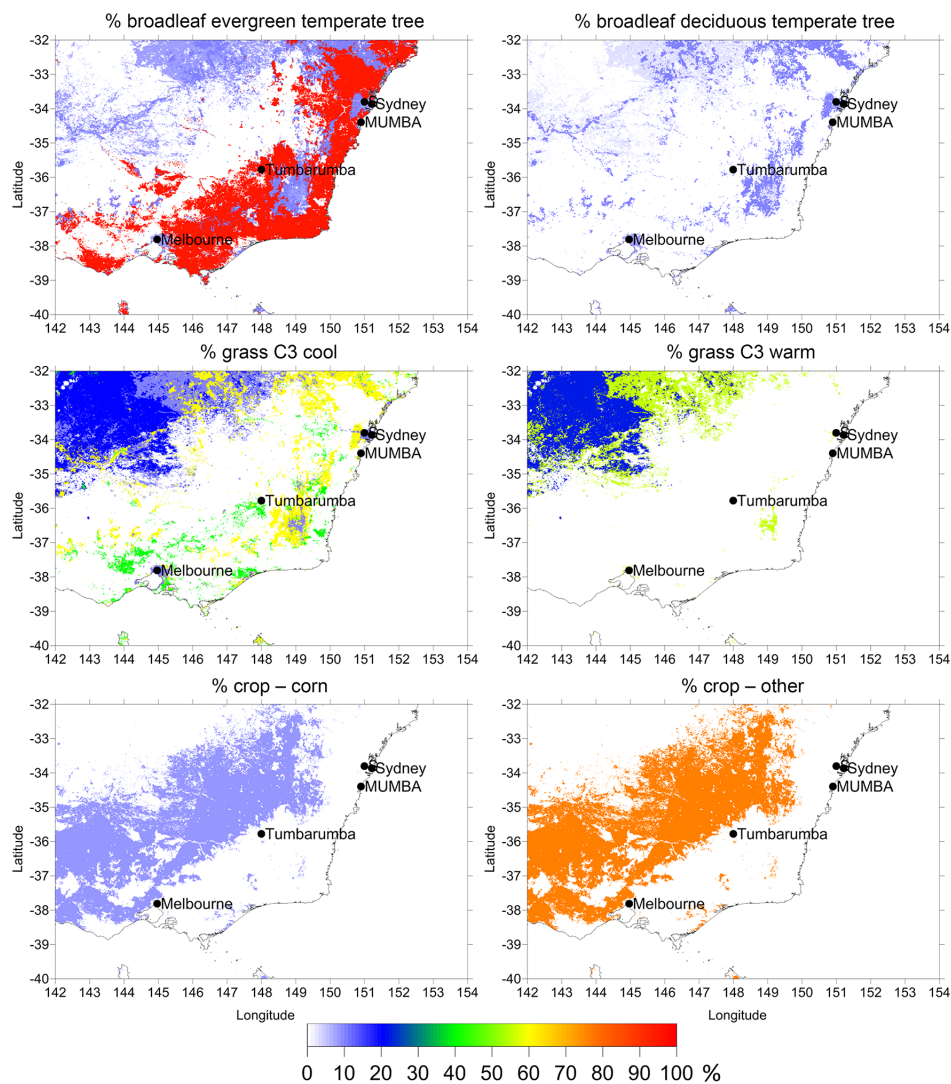
Figure 3. The percentage area covered by the indicated PFTs resulting from splitting the 1 km IGBP database into NCAR PFTs in southeast Australia.
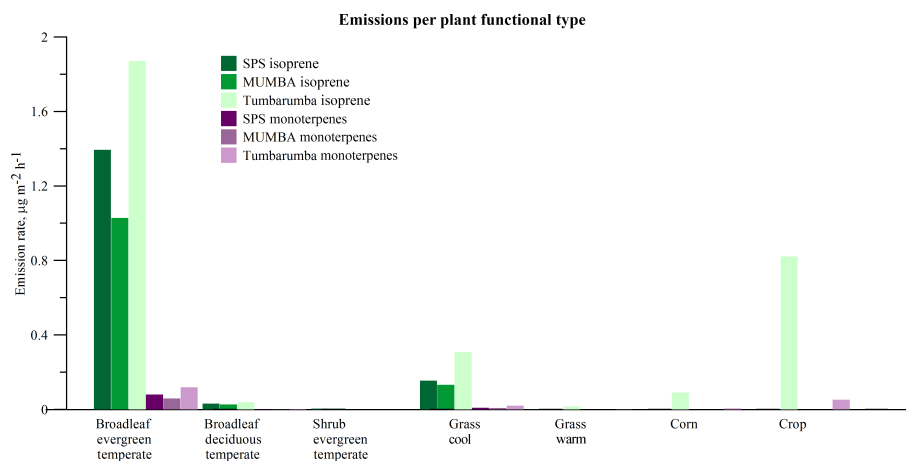

Figure 4. Emission rates of isoprene and monoterpenes per PFT within each campaign's inner domain ($180 \, \text{km} \times 180 \, \text{km}$).
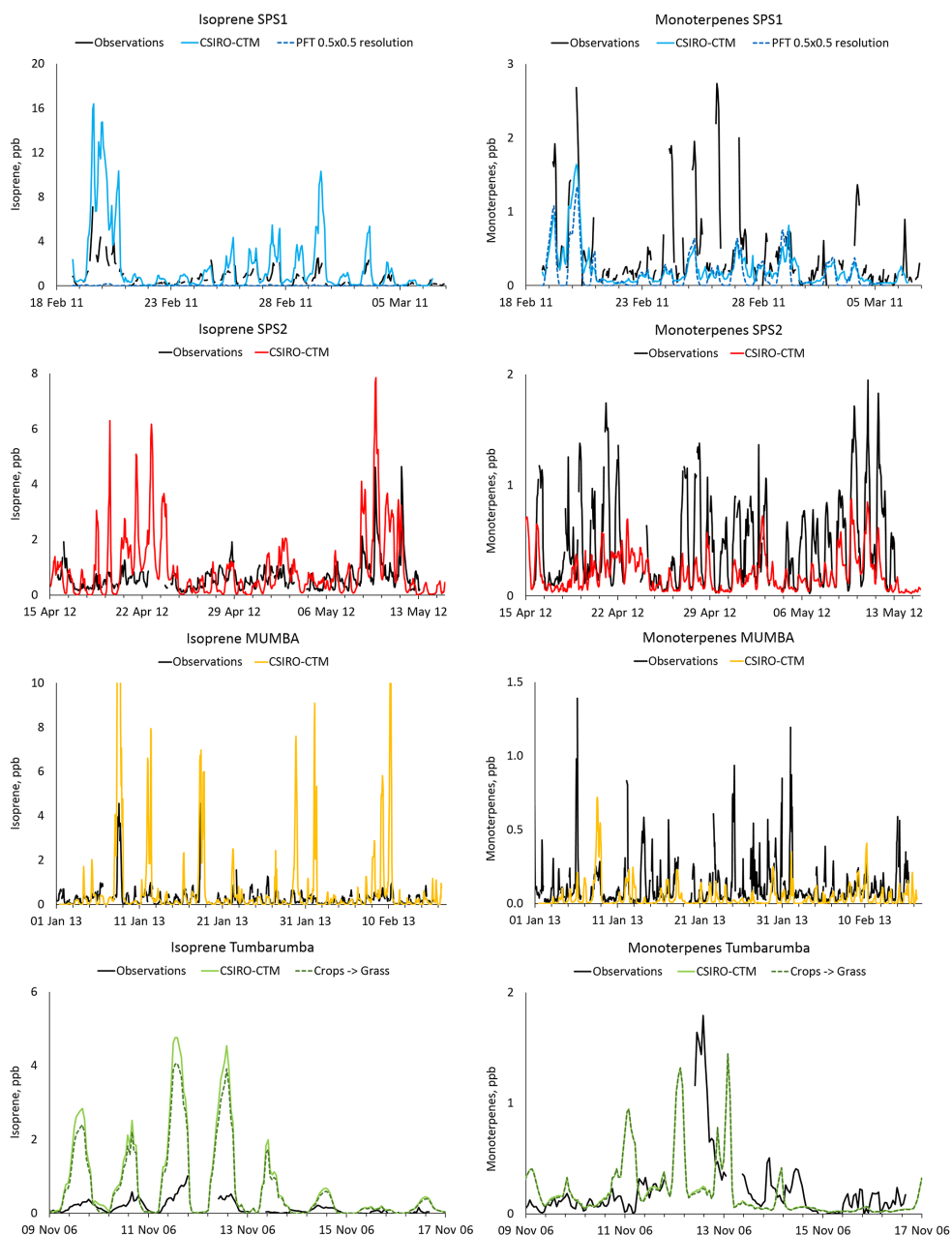
Figure 5. Time series of observed and modelled isoprene (left) and monoterpenes (right) for each field campaign. SPS1: blue; SPS2: red; MUMBA: yellow; Tumbarumba: green. The *y* axis for isoprene during MUMBA is restricted to 10 ppb, as the modelled peak is 38 ppb on 8 January 2013.

monoterpene emission fluxes would be broadly similar for both chemical species, but more measurements are needed to confirm this. The magnitudes of the average observed isoprene and monoterpene atmospheric concentrations are broadly similar for all four field studies, shown in Table 2. As atmospheric concentrations are directly related to their emission rates, the magnitudes of isoprene and monoterpene emission fluxes must be similar under normal (non-storm) conditions, and the ratio of emitted isoprene carbon

to monoterpene carbon could be ∼ 0.5–2. This phenomenon may be unique to southeast Australia.

Figure 7 shows campaign average diurnal time series for isoprene, monoterpenes and the ratio of carbon in isoprene vs. monoterpene atmospheric concentrations, comparing the CTM to the observations. In most cases the MEGAN scheme predicts the shape of the diurnal profiles well, but isoprene is over-predicted during all four field campaigns. A similar over-prediction in isoprene concentrations occurred using
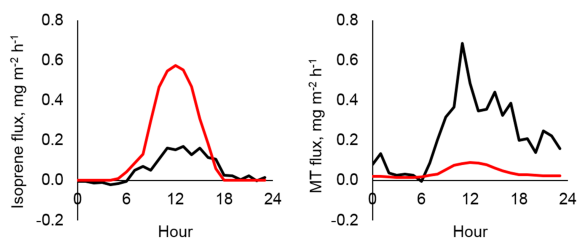
Figure 6. Diurnal cycles of isoprene (left) and monoterpene (MT, right) emission fluxes from 3 days of eddy covariance measurements at Tumbarumba during November 2006 (black). Modelled emission fluxes are plotted from the same time period (red).

Table 2. Average (min–max) observed isoprene and monoterpene concentrations at all four field sites.

Observations	Isoprene ppb	Monoterpenes ppb
SPS1	0.76	0.44
	(0.09*–7.10)	(0.20*–2.74)
SPS2	0.63	0.46
	(0.01–4.63)	(0.006–1.95)
MUMBA	0.28	0.12
	(0.002–4.57)	(0.004*–1.39)
Tumbarumba	0.15	0.20
	(0.02*–1.01)	(0.02*–1.79)

* Values equate to half the limit of detection.

the CHIMERE model, run with MEGANv2.04 at 9 km resolution during the MUMBA campaign (Paton-Walsh et al., 2016).

The peak in modelled isoprene is over-predicted by factors of between 2 and 6, which will have an effect through the chemistry dependent on oxidant availability. The modelled isoprene profile captures the observed peak at 10:00 seen at MUMBA in summer. The observed late afternoon peak in isoprene during SPS2 is diagnosed as being due to a collapsing autumnal boundary layer where oxidants at this time are depleted, but isoprene continues to be emitted.

The observed ratio of isoprene carbon vs. monoterpene carbon peaks under ∼ 2.5 at all four field studies. The model over-predicts the observed ratio by factors of between 3 and 10, the latter at MUMBA, where lower monoterpene concentrations were predicted compared with Sydney and Tumbarumba.

The modelled profile of monoterpenes generally matches the observed peaks for SPS1, SPS2 and MUMBA campaigns, but the magnitude is under-predicted particularly at night by factors of between 3 and 4. At Tumbarumba the model predicts a similar monoterpene profile (peaks at night) to the other field campaigns, but the observations show a light-dependent profile, similar to isoprene. This could indicate plant stress due to storm damage occurring that week (Harley et al., 2014). This process is not in the model.
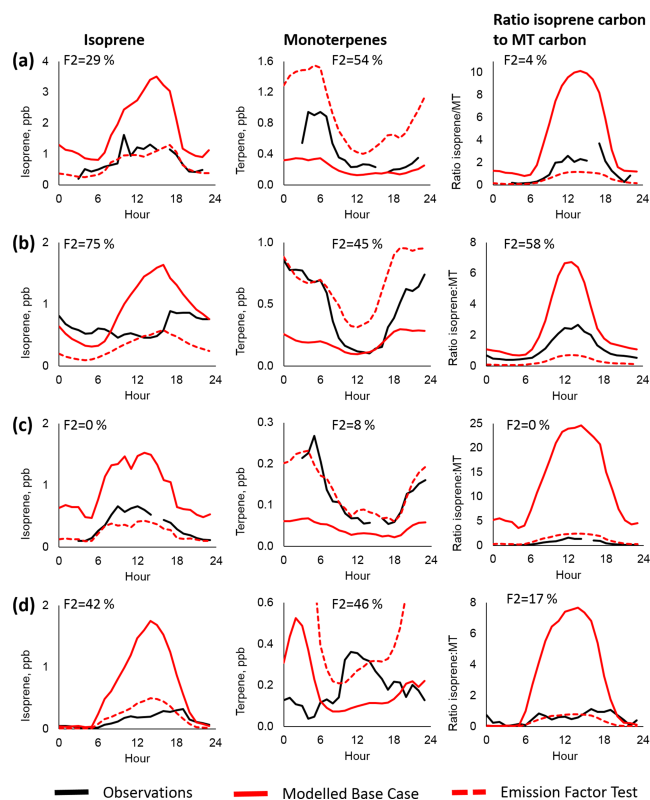

Figure 7. Campaign average diurnal cycles for isoprene (left), monoterpenes (middle) and the ratio of isoprene carbon to monoterpene (MT) carbon (right). **(a)** SPS1, **(b)** SPS2, **(c)** MUMBA and **(d)** Tumbarumba. F2: percentage within a factor of 2 between observations and base run.

Clearly, modelled isoprene is too high and monoterpenes are too low in southeast Australia. Sensitivity runs are conducted to establish the magnitudes of emission corrections needed to achieve better model–observation agreement. Emission factors for isoprene were reduced by a factor of 3. The emission factors for the monoterpenes species myrcene, sabinene, limonene, 3-carene, ocimene, α-pinene and β-pinene were increased by a factor of 3.5. Other monoterpene species remain unchanged as their concentrations do not dominate the total (Sindelarova et al., 2014). The factors chosen are somewhat arbitrary. A decrease factor of 3 for isoprene suited the SPS1 profile best, whilst an increase of 3.5 suited the MUMBA monoterpenes profile best.

The modelled diurnal cycles from the emission factor sensitivity tests are shown as dashed red lines within Fig. 7. The reduction in isoprene and increase in monoterpenes show better modelled agreement for most campaigns, but particularly for isoprene in SPS1 and monoterpenes at MUMBA. The ratio of isoprene carbon to monoterpene carbon concentrations from the emission factor sensitivity test give more reasonable results at MUMBA and Tumbarumba, but underpredict the observed ratio for SPS1 and SPS2. Reducing the
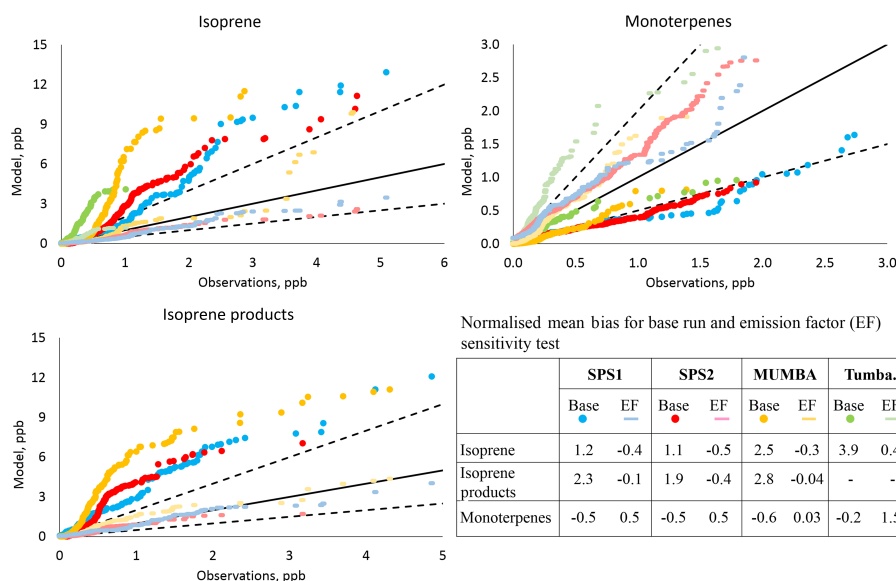
Figure 8. Quantile–quantile plots to show relationship between modelled and observed biogenic gases. The base run are dots and the emission factor sensitivity study are the dashes. The solid black line is the 1 : 1 line; dashed black lines indicate a factor of ±2. Note: isoprene products are MVK + MACR. The y axis on isoprene chart is reduced to 15 ppb to aid visual comparison, as modelled MUMBA data reach 38 ppb.

isoprene emission factors has incurred a linear response in reducing the isoprene concentrations, but the factor of 3 used is not suitable for all the field campaign data. At Tumbarumba, the reduction is likely a factor of 6. Similarly the monoterpene increase by a factor of 3.5 does not suit all Australian conditions. Nevertheless, these results indicate the magnitude of the corrections required.

Figure 8 shows quantile–quantile plots showing modelled and observed data ranked in ascending order. They highlight any systematic biases that exist in the modelled data; if the modelled data were exactly like the observations then the points would sit on the 1 : 1 line. Figure 8 shows the 1 : 1 line with two dashed lines representing a factor of 2 either side. The aim is to further examine the extent of the over/under-prediction in isoprene and monoterpenes. The data are paired; if the PTR-MS was offline then the modelled data are removed for these times. The normalised mean bias is calculated; values closer to zero exhibit less bias.

There is a large model over-prediction in isoprene and therefore the isoprene products. Note that measurements of isoprene products were not made available from Tumbarumba. The modelled monoterpenes are under-predicted by just over a factor of 2 in most cases. The one exception is Tumbarumba, which has zero model bias in monoterpenes; however, the shape of the modelled diurnal cycle was at odds with the observed profile. The results from the emission factor sensitivity test show better modelled isoprene profiles, but the factor of 3.5 increase in monoterpene emissions is too high. The bias in modelled VOCs is reduced in the emission factor sensitivity test. For isoprene the bias switches from positive to negative, indicating that the chosen decrease fac-

tor is too high. The increase factor for monoterpenes is too high for SPS1 and SPS2, both of which show equal sized biases but with the opposite sign to the bias in the base case run.

The concentrations of the isoprene products can also be used to evaluate the lifetime of isoprene in the model and observations. Figure 9 shows the ratio of isoprene and its products to the isoprene products. This examines whether the model chemistry is proceeding at observed rates. The results show high correlations (> 0.85) for the observed ratios, correlations in excess of 0.90 for SPS1 and SPS2 for species modelled by the base case run, and lower correlation (> 0.78) in the modelled base case at MUMBA. More isoprene products are predicted by the model than the observations for SPS1. This suggests that oxidation occurs faster in the model compared to the observations for February 2011. However, the modelled rates of oxidation are more reasonable for SPS2 and MUMBA. There is a slight improvement in the r^2 correlation coefficient between species modelled by the emission factor sensitivity test for SPS1 and SPS2.

4 Summary and conclusions

MEGANv2.1 has been incorporated into the CSIRO Chemical Transport Model. The CTM used a nested grid approach, downscaling from an Australia-wide domain to focus on receptor sites at a resolution of 3 km. This high-resolution simulation required a new plant functional type map to be constructed for Australia from an IGBP 1 km dataset. Whilst deconstructing the IGBP dataset to fit the NCAR PFTs has been done in accordance with literature and local knowl-
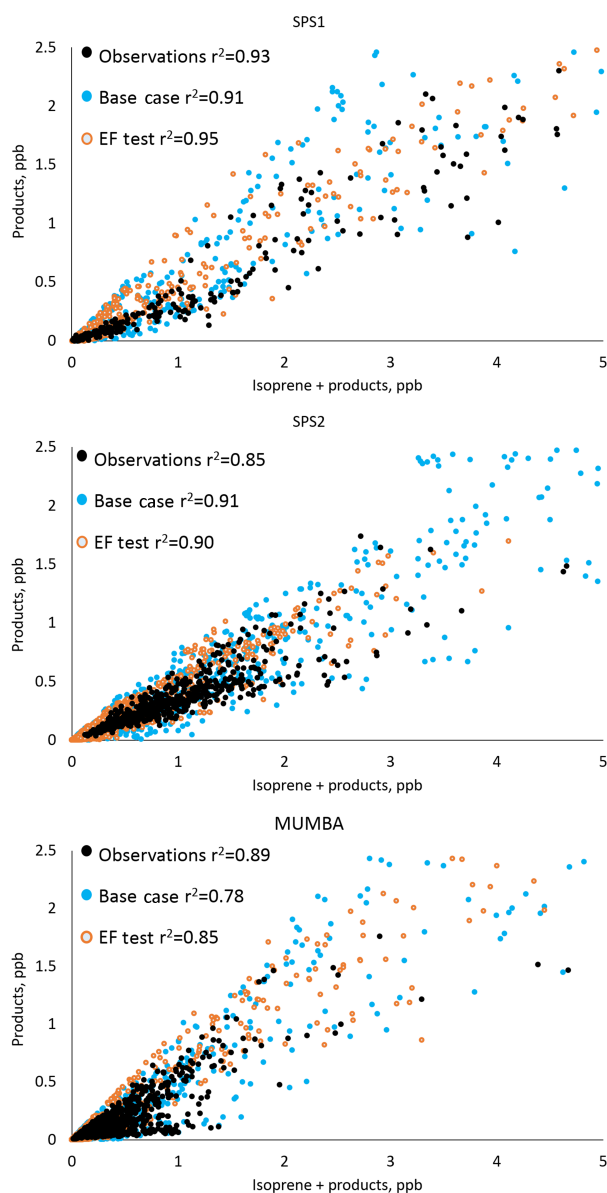
Figure 9. Scatter plots of modelled and observed ratios between isoprene and the isoprene products, with r^2 correlation coefficients. EF: emission factor sensitivity test. Note that the x and y axes are restricted to 5 and 2.5 ppb respectively.

edge, it is subjective and may have introduced uncertainty. The model was used to predict concentrations measured during four field campaigns in southeast Australia: one in spring (Tumbarumba), two in summer (SPS1 and MUMBA) and one in Autumn (SPS2). The observed concentrations of isoprene and monoterpenes were of a broadly similar magnitude, which may indicate that southeast Australia holds an unusual position where neither chemical species dominates. The model over-predicted isoprene concentrations (up to a factor of 6) and under-predicted monoterpenes (up to a factor of 4). A short series of measured emission fluxes

at Tumbarumba showed that the model over-predicted isoprene fluxes by a factor of 3 and under-predicted monoterpene fluxes by a factor of 4 at midday.

Southeast Australia is dominated by forested regions, and cities here are surrounded by a high source of BVOC emissions. These BVOCs have the capacity to dominate atmospheric chemical processes in urban airsheds during the high temperatures experienced in Australian summers. Southeast Australia has been considered a global hotspot for isoprene emissions due to the presence of high emitting eucalypt species (Guenther et al., 2012), although our results indicate that eucalypts may not emit as much isoprene as previously thought. The MEGANv2.1 isoprene and monoterpene emission factors assigned to eucalypts, 24 and $1.6\,\mathrm{mg\,m^{-2}\,h^{-1}}$ respectively, are higher than the global average value of all broadleaf evergreen temperate trees (10 and $0.99\,\mathrm{mg\,m^{-2}\,h^{-1}}$, Table 2 of Guenther et al., 2012) because not all broadleaf evergreen temperate trees have high isoprene and monoterpene emissions.

While there is a limited understanding of all of the processes controlling biogenic VOC emissions, such as the impact of droughts, which can lead to an inhibition of BVOC emissions (Sharkey and Loreto, 1993; Pegoraro et al., 2007), the overall emission can be adjusted by revising the emission factor. A sensitivity study reduced the emission factors of isoprene by 3 and increased the monoterpene emission factors by 3.5. The effects on the modelled concentrations was roughly linear. This experiment showed that there is no single increase/decrease factor which suits all locations/seasons found in southeast Australia, indicating that adjustment is needed not only in the emission factors but also in the representations of the processes controlling emissions variations.

The MEGANv2.1 emission factors for eucalyptus were primarily based on enclosure measurements of young trees. Street et al. (1997) conducted field enclosure measurements of *Eucalyptus globulus* trees in a plantation in Portugal and found that both isoprene and monoterpene emissions from a 7-year-old tree were about 5 times lower than the emissions of a year-old sapling. Nunes and Pio (2001) compared emissions from 2-year-old *Eucalyptus globulus* saplings in the laboratory and 7-year-old trees in a plantation and found the adult tree isoprene emissions were about a third lower than that of the young tree. The isoprene emission rates of adult *E. globulus*, *E. grandis* and *E. camaldulensis* trees measured by Winters et al. (2009) are a factor of 4 lower than the emissions that He et al. (2000) measured from 2-year-old potted saplings of the same three eucalypt species. This is in good agreement with the results of Street et al. (1997) and Nunes and Pio (2001). The monoterpene emission rates measured by Winters et al. (2009) for adult trees, however, were a factor of 4 higher than the 2-year-old saplings measured by He et al. (2000). This does not agree with the findings of Street et al. (1997), but it does agree with the higher than predicted atmospheric concentration measured at the field sites described in this paper. These results suggest that the

MEGANv2.1 isoprene emission factors for eucalypts are biased by being based on measurements of young trees and should be decreased by up to a factor of 4 or 5 considering that the isoprene-emitting canopy consists primarily of adult trees. This would result in better agreement with the observed ambient isoprene concentrations described above. The results of monoterpene enclosure studies are more inconclusive and are also difficult to interpret due to artefacts associated with elevated emissions from disturbance of the monoterpene storage structures (Winters et al., 2009).

In order to more accurately characterise the atmospheric chemistry, air quality and climate in Australia, further observations and quantitative analysis of Australian BVOC emission rates are needed. Australia is biologically diverse and the canopy and understory are composed of many other species in addition to eucalypts. Satellite column measurements of BVOC oxidation products such as formaldehyde and glyoxal are available and can be useful for investigating regional and seasonal distributions of biogenic emissions (Palmer et al., 2003; Kaiser et al., 2015). Direct flux measurements, using towers and aircraft eddy flux approaches, are needed to provide a direct constraint on Australian BVOC emissions (Karl et al., 2013).

Data availability

The LAI data product was retrieved from MCD15A2 version 4 from the online Data Pool, courtesy of the NASA Land Processes Distributed Active Archive Center (LP DAAC), USGS/Earth Resources Observation and Science (EROS) Center, Sioux Falls, South Dakota, https://lpdaac.usgs.gov/data_access/data_pool. The Australian tree/shrub composition dataset is from the Department of Agriculture, DAWR 2003, Forests of Australia 2003, Department of Agriculture and Water Resources, Australia: http://data.gov.au/dataset/forests-of-australia-2003. Average winter temperature data available from the Bureau of Meteorology, Australia: http://www.bom.gov.au/jsp/awap/.

The Supplement related to this article is available online at doi:10.5194/acp-16-6997-2016-supplement.

References

Arneth, A., Schurgers, G., Lathiere, J., Duhl, T., Beerling, D. J., Hewitt, C. N., Martin, M., and Guenther, A.: Global terrestrial isoprene emission models: sensitivity to variability in climate and vegetation, Atmos. Chem. Phys., 11, 8037–8052, doi:10.5194/acp-11-8037-2011, 2011.

Ashworth, K., Wild, O., and Hewitt, C. N.: Sensitivity of isoprene emissions estimated using MEGAN to the time resolution of input climate data, Atmos. Chem. Phys., 10, 1193–1201, doi:10.5194/acp-10-1193-2010, 2010.

Ayers, G. P. and Gillett, R. W.: Isoprene Emissions from Vegetation and Hydrocarbon Emissions from Bushfires in Tropical Australia, J. Atmos. Chem., 7, 177–190, doi:10.1007/Bf00048045, 1988.

Belward, A. S., Estes, J. E., and Kline, K. D.: The IGBP-DIS global 1-km land-cover data set DISCover: A project overview, Photogramm. Eng. Rem. S., 65, 1013–1020, 1999.

BoM: High resolution monthly and multi-monthly temperature gridded datasets from 1911 onwards, Bureau of Meteorology, Australia, available at: http://www.bom.gov.au/jsp/awap/, last access: 2009.

Bonan, G. B., Levis, S., Kergoat, L., and Oleson, K. W.: Landscapes as patches of plant functional types: An integrating concept for climate and ecosystem models, Global Biogeochem. Cy., 16, 1021, doi:10.1029/2000gb001360, 2002.

Cope, M., Keywood, M., Emmerson, K., Galbally, I., Boast, K., Chambers, S., Cheng, M., Crumeyrolle, S., Dunne, E., Fedele, F., Gillett, R. W., Griffiths, A., Harnwell, J., Katzfey, J., Hess, D., Lawson, S., Miljevic, B., Molloy, S., Powell, J., Reisen, F., Ristovski, Z., Selleck, P., Ward, J., Zhang, C., and Seng, J.: The Sydney Particle Study. CSIRO, Australia, available at: http://www.environment.nsw.gov.au/aqms/sydparticlestudy.htm (last access: 2 June 2016), 2014.

Cope, M. E., Hess, G. D., Lee, S., Tory, K., Azzi, M., Carras, J., Lilley, W., Manins, P. C., Nelson, P., Ng, L., Puri, K., Wong, N., Walsh, S., and Young, M.: The Australian Air Quality Forecasting System. Part I: Project description and early outcomes, J. Appl. Meteorol., 43, 649–662, doi:10.1175/2093.1, 2004.

Corney, S., Grose, M., Bennett, J. C., White, C., Katzfey, J., McGregor, J., Holz, G., and Bindoff, N. L.: Performance of downscaled regional climate simulations using a variable-resolution regional climate model: Tasmania as a test case, J. Geophys. Res.-Atmos., 118, 11936–11950, doi:10.1002/2013jd020087, 2013.

DAWR: Forests of Australia 2003, Department of Agriculture and Water Resources, Australia, available at: https://data.gov.au/datsaset/forests-of-australia-2003 (last access: 2004), 2003.

DECCW: Air emissions inventory for the Greater Metropolitan Region in New South Wales; Calendar year 2003, Sydney South, Australia, 2007.

Emmerson, K. M. and Evans, M. J.: Comparison of tropospheric gas-phase chemistry schemes for use within global models, Atmos. Chem. Phys., 9, 1831–1845, doi:10.5194/acp-9-1831-2009, 2009.

Emmons, L. K., Walters, S., Hess, P. G., Lamarque, J.-F., Pfister, G. G., Fillmore, D., Granier, C., Guenther, A., Kinnison, D., Laepple, T., Orlando, J., Tie, X., Tyndall, G., Wiedinmyer, C., Baughcum, S. L., and Kloster, S.: Description and evaluation of the Model for Ozone and Related chemical Tracers, version 4

(MOZART-4), Geosci. Model Dev., 3, 43–67, doi:10.5194/gmd-3-43-2010, 2010.

Evans, R. C., Tingey, D. T., Gumpertz, M. L., and Burns, W. F.: Estimates of isoprene and monoterpene emissions rates in plants, Bot. Gaz., 143, 304–310, 1982.

Fountoukis, C. and Nenes, A.: ISORROPIA II: a computationally efficient thermodynamic equilibrium model for K^+–Ca^{2+}–Mg^{2+}–NH_4^+–Na^+–SO_4^{2-}–NO_3^-–Cl^-–H_2O aerosols, Atmos. Chem. Phys., 7, 4639–4659, doi:10.5194/acp-7-4639-2007, 2007.

Greenberg, J. P., Guenther, A. B., Petron, G., Wiedinmyer, C., Vega, O., Gatti, L. V., Tota, J., and Fisch, G.: Biogenic VOC emissions from forested Amazonian landscapes, Glob. Change Biol., 10, 651–662, doi:10.1111/j.1365-2486.2004.00758.x, 2004.

Griffin, R. J., Cocker, D. R., Seinfeld, J. H., and Dabdub, D.: Estimate of global atmospheric organic aerosol from oxidation of biogenic hydrocarbons, Geophys. Res. Lett., 26, 2721–2724, doi:10.1029/1999gl900476, 1999.

Guenther, A., Hewitt, C. N., Erickson, D., Fall, R., Geron, C., Graedel, T., Harley, P., Klinger, L., Lerdau, M., Mckay, W. A., Pierce, T., Scholes, B., Steinbrecher, R., Tallamraju, R., Taylor, J., and Zimmerman, P.: A Global-Model of Natural Volatile Organic-Compound Emissions, J. Geophys. Res.-Atmos., 100, 8873–8892, doi:10.1029/94jd02950, 1995.

Guenther, A., Otter, L., Zimmerman, P., Greenberg, J., Scholes, R., and Scholes, M.: Biogenic hydrocarbon emissions from southern African savannas, J. Geophys. Res.-Atmos., 101, 25859–25865, doi:10.1029/96jd02597, 1996.

Guenther, A., Archer, S., Greenberg, J., Harley, P., Helmig, D., Klinger, L., Vierling, L., Wildermuth, M., Zimmerman, P., and Zitzer, S.: Biogenic hydrocarbon emissions and land-cover/climate change in a subtropical savanna, Phys. Chem. Earth Pt. B, 24, 659–667, doi:10.1016/S1464-1909(99)00062-3, 1999.

Guenther, A., Karl, T., Harley, P., Wiedinmyer, C., Palmer, P. I., and Geron, C.: Estimates of global terrestrial isoprene emissions using MEGAN (Model of Emissions of Gases and Aerosols from Nature), Atmos. Chem. Phys., 6, 3181–3210, doi:10.5194/acp-6-3181-2006, 2006.

Guenther, A. B., Monson, R. K., and Fall, R.: Isoprene and Monoterpene Emission Rate Variability – Observations with Eucalyptus and Emission Rate Algorithm Development, J. Geophys. Res.-Atmos., 96, 10799–10808, doi:10.1029/91jd00960, 1991.

Guenther, A. B., Jiang, X., Heald, C. L., Sakulyanontvittaya, T., Duhl, T., Emmons, L. K., and Wang, X.: The Model of Emissions of Gases and Aerosols from Nature version 2.1 (MEGAN2.1): an extended and updated framework for modeling biogenic emissions, Geosci. Model Dev., 5, 1471–1492, doi:10.5194/gmd-5-1471-2012, 2012.

Harley, P., Otter, L., Guenther, A., and Greenberg, J.: Micrometeorological and leaf-level measurements of isoprene emissions from a southern African savanna, J. Geophys. Res.-Atmos., 108, 8468 doi:10.1029/2002jd002592, 2003.

Harley, P., Eller, A., Guenther, A., and Monson, R. K.: Observations and models of emissions of volatile terpenoid compounds from needles of ponderosa pine trees growing in situ: control by light, temperature and stomatal conductance, Oecologia, 176, 35–55, doi:10.1007/s00442-014-3008-5, 2014.

He, C. R., Murray, F., and Lyons, T.: Monoterpene and isoprene emissions from 15 Eucalyptus species in Australia, Atmos. Environ., 34, 645–655, doi:10.1016/S1352-2310(99)00219-8, 2000.

Heald, C. L., Henze, D. K., Horowitz, L. W., Feddema, J., Lamarque, J. F., Guenther, A., Hess, P. G., Vitt, F., Seinfeld, J. H., Goldstein, A. H., and Fung, I.: Predicted change in global secondary organic aerosol concentrations in response to future climate, emissions, and land use change, J. Geophys. Res., 113, D05211, doi:10.1029/2007jd009092, 2008.

Heald, C. L., Wilkinson, M. J., Monson, R. K., Alo, C. A., Wang, G. L., and Guenther, A.: Response of isoprene emission to ambient CO_2 changes and implications for global budgets, Glob. Change Biol., 15, 1127–1140, doi:10.1111/j.1365-2486.2008.01802.x, 2009.

Hoffmann, T., Odum, J. R., Bowman, F., Collins, D., Klockow, D., Flagan, R. C., and Seinfeld, J. H.: Formation of organic aerosols from the oxidation of biogenic hydrocarbons, J. Atmos. Chem., 26, 189–222, doi:10.1023/A:1005734301837, 1997.

Houweling, S., Dentener, F., and Lelieveld, J.: The impact of nonmethane hydrocarbon compounds on tropospheric photochemistry, J. Geophys. Res.-Atmos., 103, 10673–10696, doi:10.1029/97jd03582, 1998.

Kaiser, J., Wolfe, G. M., Min, K. E., Brown, S. S., Miller, C. C., Jacob, D. J., deGouw, J. A., Graus, M., Hanisco, T. F., Holloway, J., Peischl, J., Pollack, I. B., Ryerson, T. B., Warneke, C., Washenfelder, R. A., and Keutsch, F. N.: Reassessing the ratio of glyoxal to formaldehyde as an indicator of hydrocarbon precursor speciation, Atmos. Chem. Phys., 15, 7571–7583, doi:10.5194/acp-15-7571-2015, 2015.

Kanawade, V. P., Jobson, B. T., Guenther, A. B., Erupe, M. E., Pressley, S. N., Tripathi, S. N., and Lee, S.-H.: Isoprene suppression of new particle formation in a mixed deciduous forest, Atmos. Chem. Phys., 11, 6013–6027, doi:10.5194/acp-11-6013-2011, 2011.

Karl, T., Misztal, P. K., Jonsson, H. H., Shertz, S., Goldstein, A. H., and Guenther, A. B.: Airborne Flux Measurements of BVOCs above Californian Oak Forests: Experimental Investigation of Surface and Entrainment Fluxes, OH Densities, and Damkohler Numbers, J. Atmos. Sci., 70, 3277–3287, doi:10.1175/Jas-D-13-054.1, 2013.

Kim, H.-K., Woo, J.-H., Park, R. S., Song, C. H., Kim, J.-H., Ban, S.-J., and Park, J.-H.: Impacts of different plant functional types on ambient ozone predictions in the Seoul Metropolitan Areas (SMAs), Korea, Atmos. Chem. Phys., 14, 7461–7484, doi:10.5194/acp-14-7461-2014, 2014.

Kirstine, W., Galbally, I., Ye, Y. R., and Hooper, M.: Emissions of volatile organic compounds (primarily oxygenated species) from pasture, J. Geophys. Res.-Atmos., 103, 10605–10619, doi:10.1029/97jd03753, 1998.

Kirstine, W. V. and Galbally, I. E.: A simple model for estimating emissions of volatile organic compounds from grass and cut grass in urban airsheds and its application to two Australian cities, J. Air Waste Manage., 54, 1299–1311, 2004.

Knote, C., Tuccella, P., Curci, G., Emmons, L., Orlando, J. J., Madronich, S., Baro, R., Jimenez-Guerrero, P., Luecken, D., Hogrefe, C., Forkel, R., Werhahn, J., Hirtl, M., Perez, J. L., San Jose, R., Giordano, L., Brunner, D., Yahya, K., and Zhang, Y.: Influence of the choice of gas-phase mechanism on predictions of key gaseous pollutants during the

AQMEII phase-2 intercomparison, Atmos. Environ., 115, 553–568, doi:10.1016/j.atmosenv.2014.11.066, 2015.

Kowalczyk, E. A., Stevens, L., Law, R. M., Dix, M., Wang, Y. P., Harman, I. N., Haynes, K., Srbinovsky, J., Pak, B., and Ziehn, T.: The land surface model component of ACCESS: description and impact on the simulated surface climatology, Aust. Meteorol. Ocean, 63, 65–82, 2013.

Lathière, J., Hauglustaine, D. A., Friend, A. D., De Noblet-Ducoudré, N., Viovy, N., and Folberth, G. A.: Impact of climate variability and land use changes on global biogenic volatile organic compound emissions, Atmos. Chem. Phys., 6, 2129–2146, doi:10.5194/acp-6-2129-2006, 2006.

Lee, A., Schade, G. W., Holzinger, R., and Goldstein, A. H.: A comparison of new measurements of total monoterpene flux with improved measurements of speciated monoterpene flux, Atmos. Chem. Phys., 5, 505–513, doi:10.5194/acp-5-505-2005, 2005.

Loreto, F. and Delfine, S.: Emission of isoprene from salt-stressed Eucalyptus globulus leaves, Plant Physiol., 123, 1605–1610, doi:10.1104/pp.123.4.1605, 2000.

Maleknia, S. D.: Mass spectrometry's role in studies of volatile organic pollutants, in: Comprehensive environmental mass spectrometry, edited by: Lebedev, A. T., ILM Publications, Hertfordshire, UK, 2012.

Maleknia, S. D., Bell, T. L., and Adams, M. A.: Eucalypt smoke and wildfires: Temperature dependent emissions of biogenic volatile organic compounds, Int. J. Mass Spectrom., 279, 126–133, doi:10.1016/j.ijms.2008.10.027, 2009.

McGregor, J. L. and Dix, M. R.: An updated description of the Conformal-Cubic atmospheric model, in: High Resolution Numerical Modelling of the Atmosphere and Ocean, edited by: Hamilton, K. and Ohfuchi, W., Springer, 51–75, doi:10.1007/978-0-387-49791-4_4, 2008.

Millet, D. B., Guenther, A., Siegel, D. A., Nelson, N. B., Singh, H. B., de Gouw, J. A., Warneke, C., Williams, J., Eerdekens, G., Sinha, V., Karl, T., Flocke, F., Apel, E., Riemer, D. D., Palmer, P. I., and Barkley, M.: Global atmospheric budget of acetaldehyde: 3-D model analysis and constraints from in-situ and satellite observations, Atmos. Chem. Phys., 10, 3405–3425, doi:10.5194/acp-10-3405-2010, 2010.

Müller, J.-F., Stavrakou, T., Wallens, S., De Smedt, I., Van Roozendael, M., Potosnak, M. J., Rinne, J., Munger, B., Goldstein, A., and Guenther, A. B.: Global isoprene emissions estimated using MEGAN, ECMWF analyses and a detailed canopy environment model, Atmos. Chem. Phys., 8, 1329–1341, doi:10.5194/acp-8-1329-2008, 2008.

Nguyen, K. C., Katzfey, J. J., and McGregor, J. L.: Downscaling over Vietnam using the stretched-grid CCAM: verification of the mean and interannual variability of rainfall, Clim. Dynam., 43, 861–879, doi:10.1007/s00382-013-1976-5, 2014.

Nunes, T. V. and Pio, C. A.: Emission of volatile organic compounds from Portuguese Eucalyptus forests, Chemosphere – Global Change Science, 3, 239–248, 2001.

Palmer, P. I., Jacob, D. J., Fiore, A. M., Martin, R. V., Chance, K., and Kurosu, T. P.: Mapping isoprene emissions over North America using formaldehyde column observations from space, J. Geophys. Res.-Atmos., 108, 4180, doi:10.1029/2002jd002153, 2003.

Papiez, M. R., Potosnak, M. J., Goliff, W. S., Guenther, A. B., Matsunaga, S. N., and Stockwell, W. R.: The impacts of reactive terpene emissions from plants on air qual-

ity in Las Vegas, Nevada, Atmos. Environ., 43, 4109–4123, doi:10.1016/j.atmosenv.2009.05.048, 2009.

Paton-Walsh, C., Guerette, E.-A., Kubiston, D., Humphries, R., Wilson, S., Rea, G., Shi, X., Griffith, D., Buchholz, R., Dominick, D., Velazco, V., Galbally, I., Keywood, M., Lawson, S., Selleck, P., Cheng, M., Molloy, S., Bhujel, M., Emmerson, K., Griffiths, A., Chambers, S., and Davy, P.: Overview of the MUMBA campaign: Measurements of Urban, Marine and Biogenic Air, Atmos. Environ., in review, 2016.

Pegoraro, E., Potosnak, M. J., Monson, R. K., Rey, A., Barron-Gafford, G., and Osmond, C. B.: The effect of elevated CO_2, soil and atmospheric water deficit and seasonal phenology on leaf and ecosystem isoprene emission, Funct. Plant Biol., 34, 774–784, doi:10.1071/Fp07021, 2007.

Pfister, G. G., Emmons, L. K., Hess, P. G., Lamarque, J. F., Orlando, J. J., Walters, S., Guenther, A., Palmer, P. I., and Lawrence, P. J.: Contribution of isoprene to chemical budgets: A model tracer study with the NCAR CTM MOZART-4, J. Geophys. Res.-Atmos., 113, D05308, doi:10.1029/2007jd008948, 2008.

Pierce, T., Geron, C., Bender, L., Dennis, R., Tonnesen, G., and Guenther, A.: Influence of increased isoprene emissions on regional ozone modeling, J. Geophys. Res.-Atmos., 103, 25611–25629, doi:10.1029/98jd01804, 1998.

Poulter, B., Ciais, P., Hodson, E., Lischke, H., Maignan, F., Plummer, S., and Zimmermann, N. E.: Plant functional type mapping for earth system models, Geosci. Model Dev., 4, 993–1010, doi:10.5194/gmd-4-993-2011, 2011.

Pugh, T. A. M., Ashworth, K., Wild, O., and Hewitt, C. N.: Effects of the spatial resolution of climate data on estimates of biogenic isoprene emissions, Atmos. Environ., 70, 1–6, doi:10.1016/j.atmosenv.2013.01.001, 2013.

Sarwar, G., Luecken, D., Yarwood, G., Whitten, G. Z., and Carter, W. P. L.: Impact of an updated carbon bond mechanism on predictions from the CMAQ modeling system: Preliminary assessment, J. Appl. Meteorol. Clim, 47, 3–14, doi:10.1175/2007jamc1393.1, 2008.

Sarwar, G., Appel, K. W., Carlton, A. G., Mathur, R., Schere, K., Zhang, R., and Majeed, M. A.: Impact of a new condensed toluene mechanism on air quality model predictions in the US, Geosci. Model Dev., 4, 183–193, doi:10.5194/gmd-4-183-2011, 2011.

Sharkey, T. D. and Loreto, F.: Water-Stress, Temperature, and Light Effects on the Capacity for Isoprene Emission and Photosynthesis of Kudzu Leaves, Oecologia, 95, 328–333, doi:10.1007/Bf00320984, 1993.

Shrivastava, M. K., Lane, T. E., Donahue, N. M., Pandis, S. N., and Robinson, A. L.: Effects of gas particle partitioning and aging of primary emissions on urban and regional organic aerosol concentrations, J. Geophys. Res., 113, D18301, doi:10.1029/2007jd009735, 2008.

Simpson, D.: Biogenic Emissions in Europe, 2. Implications for Ozone Control Strategies, J. Geophys. Res.-Atmos., 100, 22891–22906, doi:10.1029/95jd01878, 1995.

Sindelarova, K., Granier, C., Bouarar, I., Guenther, A., Tilmes, S., Stavrakou, T., Müller, J.-F., Kuhn, U., Stefani, P., and Knorr, W.: Global data set of biogenic VOC emissions calculated by the MEGAN model over the last 30 years, Atmos. Chem. Phys., 14, 9317–9341, doi:10.5194/acp-14-9317-2014, 2014.

Situ, S., Guenther, A., Wang, X., Jiang, X., Turnipseed, A., Wu, Z., Bai, J., and Wang, X.: Impacts of seasonal and regional variability in biogenic VOC emissions on surface ozone in the Pearl River delta region, China, Atmos. Chem. Phys., 13, 11803–11817, doi:10.5194/acp-13-11803-2013, 2013.

Spirig, C., Guenther, A., Greenberg, J. P., Calanca, P., and Tarvainen, V.: Tethered balloon measurements of biogenic volatile organic compounds at a Boreal forest site, Atmos. Chem. Phys., 4, 215–229, doi:10.5194/acp-4-215-2004, 2004.

Stavrakou, T., Müller, J.-F., Bauwens, M., De Smedt, I., Van Roozendael, M., Guenther, A., Wild, M., and Xia, X.: Isoprene emissions over Asia 1979–2012: impact of climate and land-use changes, Atmos. Chem. Phys., 14, 4587–4605, doi:10.5194/acp-14-4587-2014, 2014.

Stavrakou, T., Müller, J.-F., Bauwens, M., De Smedt, I., Van Roozendael, M., De Mazière, M., Vigouroux, C., Hendrick, F., George, M., Clerbaux, C., Coheur, P.-F., and Guenther, A.: How consistent are top-down hydrocarbon emissions based on formaldehyde observations from GOME-2 and OMI?, Atmos. Chem. Phys., 15, 11861–11884, doi:10.5194/acp-15-11861-2015, 2015.

Street, R. A., Hewitt, C. N., and Mennicken, S.: Isoprene and monoterpene emissions from a Eucalyptus plantation in Portugal, J. Geophys. Res.-Atmos., 102, 15875–15887, doi:10.1029/97jd00010, 1997.

Taraborrelli, D., Lawrence, M. G., Crowley, J. N., Dillon, T. J., Gromov, S., Gross, C. B. M., Vereecken, L., and Lelieveld, J.: Hydroxyl radical buffered by isoprene oxidation over tropical forests, Nat. Geosci., 5, 190–193, doi:10.1038/Ngeo1405, 2012

van Donkelaar, A., Martin, R. V., Park, R. J., Heald, C. L., Fu, T. M., Liao, H., and Guenther, A.: Model evidence for a significant source of secondary organic aerosol from isoprene, Atmos. Environ., 41, 1267–1274, doi:10.1016/j.atmosenv.2006.09.051, 2007.

Winer, A. M., Fitz, D. R., Miller, P. R., Atkinson, R. W., Brown, D. E., Carter, W. P. L., Dodd, M. C., Johnson, C. W., Myers, M. A., Neisess, K. R., Poe, M. P., and Stephens, E. R.: Investigation of the role of natural hydrocarbons in photochemical smog formation in California, final report contract AO-056-32, California Air Resources Board, Sacramento, California, USA, February 1983.

Winters, A. J., Adams, M. A., Bleby, T. M., Rennenberg, H., Steigner, D., Steinbrecher, R., and Kreuzwieser, J.: Emissions of isoprene, monoterpene and short-chained carbonyl compounds from Eucalyptus spp. in southern Australia, Atmos. Environ., 43, 3035–3043, doi:10.1016/j.atmosenv.2009.03.026, 2009.

Zhang, H. Q., Pak, B., Wang, Y. P., Zhou, X. Y., Zhang, Y. Q., and Zhang, L.: Evaluating Surface Water Cycle Simulated by the Australian Community Land Surface Model (CABLE) across Different Spatial and Temporal Domains, J. Hydrometeorol., 14, 1119–1138, doi:10.1175/Jhm-D-12-0123.1, 2013.